Periodontal tissue regeneration by recombinant human collagen peptide granules applied with β-tricalcium phosphate fine particles

Yuto Yoshino[1], Hirofumi Miyaji[1*], Erika Nishida[1], Yukimi Kanemoto[1], Asako Hamamoto[1], Akihito Kato[1], Tsutomu Sugaya[1], Tsukasa Akasaka[2]

[1] Department of Periodontology and Endodontology, Faculty of Dental Medicine, Hokkaido University, Sapporo, Hokkaido, Japan

[2] Department of Biomedical Materials and Engineering, Faculty of Dental Medicine, Hokkaido University, Sapporo, Hokkaido, Japan

***Corresponding author:**

Hirofumi MIYAJI

Department of Periodontology and Endodontology

Faculty of Dental Medicine, Hokkaido University

N13, W7, Kita-ku, Sapporo, Hokkaido 060-8586, Japan

E-mail: miyaji@den.hokudai.ac.jp

Abstract

Objectives

Recombinant human collagen peptide (RCP) is a recombinantly created xeno-free biomaterial enriched in arginine-glycine-aspartic acid sequences with good processability whose use for regenerative medicine applications is under investigation. The biocompatibility and osteogenic ability of RCP granules combined with β-tricalcium phosphate (TCP) submicron particles (β-TCP/RCP) were recently demonstrated. In the present study, β-TCP/RCP was implanted into experimental periodontal tissue defects created in beagles to investigate its regenerative effects.

Methods

An RCP solution was lyophilized, granulated, and thermally cross-linked into particles approximately 1 mm in diameter. β-TCP dispersion (1 wt%; 500 μL) was added to 100 mg of RCP granules to form β-TCP/RCP. A three-walled intrabony defect (5 mm × 3 mm × 4 mm) was created on the mesial side of the mandibular first molar and filled with β-TCP/RCP.

Results

A micro-computed tomography image analysis performed at 8 weeks postoperative showed a significantly greater amount of new bone after β-TCP/RCP grafting (2.2-fold, $P<0.05$) than after no grafting. Histological findings showed that the transplanted β-TCP/RCP induced active bone-like tissue formation including tartaric acid-resistant acid phosphatase– and OCN-positive cells as well as bioabsorbability. Ankylosis did not occur, and periostin-positive periodontal ligament-like tissue formation was observed. Histological measurements performed at 8 weeks postoperative revealed that β-TCP/RCP implantation formed 1.7-fold more bone-like tissue and 2.1-fold more periodontal ligament-like tissue than the control condition and significantly suppressed gingival recession and epithelial downgrowth ($P<0.05$).

Conclusions

β-TCP/RCP implantation promoted bone-like and periodontal ligament–like tissue formation, suggesting its efficacy as a periodontal tissue regenerative material.

Keywords

Beagle dog; experimental periodontal tissue defect; immunohistochemistry; micro computed tomography (CT); three-wall intrabony defect

Abbreviations

CT, computed tomography; Ctrl, control; FT, fibrous tissue; HE, hematoxylin eosin; MT, Masson's trichrome; OCN, osteocalcin; POSTIN, periostin; RCP, recombinant human collagen peptide; RGD, arginine-glycine-aspartic acid; ROI, region of interest; TCP, tricalcium phosphate; TRAP, tartaric acid-resistant acid phosphatase

1 Introduction

Periodontal regenerative therapy was developed to regenerate periodontal attachments, such as the periodontal ligament, cementum, and alveolar bone, lost due to severe periodontitis [1, 2, 3]. Various materials have been used as scaffolds for periodontal tissue regenerative therapy, in particular, the natural polymer collagen has excellent biocompatibility and bioabsorbability [4, 5]. However, commercially available collagen scaffolds are derived from domestic animal tissues, such as cows and pigs, and have the risk of bio-contamination and antigenicity, and are currently not a completely safe and secure medical material for use in humans [6]. Against this backdrop, recombinant human collagen peptide (RCP), based on the human type I collagen (α1 chain), was recently created to circumvent the problems associated with animal-derived collagen [7].

RCP is recombinantly produced by yeast to lack animal-derived components (xeno-free) and designed with an amino acid sequence that does not contain antigenic moieties. Compared to natural collagen, RCP contains more arginine-glycine-aspartic acid (RGD) sequences, which are important for cell adhesion and differentiation [8]. Like natural collagen, RCP can be processed to many forms by cross-linking and exhibits bioabsorbable properties in the body; therefore, RCP has great potential as a scaffold material *in vivo* [9, 10]. Several studies have shown that a sponge made from RCP exhibits good properties as a scaffold for bone marrow stromal cells and adipose-derived stem cells [11, 12].

However, collagen-based scaffolds generally suffer from low osteoconductive capacity compared to bioceramic materials [13]. Therefore, a combination of collagen and various bioceramics has been investigated to increase the amount of bone formation. Murakami *et al*. combined bovine-derived collagen scaffolds with fine (submicron scale) particle β-tricalcium phosphate (TCP) [14]. The composite scaffold was effective in periodontal tissue reconstruction in a canine experimental periodontal defect model [15]. Combinations with collagen and other types of bioceramics, such as octacalcium phosphate or low-crystalline hydroxyapatite, also showed excellent bone or periodontal tissue forming effects [16, 17, 18, 19]. Based on these studies, Furihata *et al*. prepared RCP granules with β-TCP fine particles (β-TCP/RCP) and showed a significant promotion of osteoblast growth and differentiation, as well as *in vivo* (in rat) bone formation, compared to normally granulated RCP (without β-TCP) [20]. Therefore, we hypothesized that β-TCP/RCP represents a promising scaffold material for periodontal tissue engineering. The purpose of this study was to evaluate the effect of β-TCP/RCP on periodontal tissue reconstruction. β-TCP/RCP was implanted into periodontal tissue defects (three-wall intrabony defects) created in the canine mandible, and reconstruction of periodontal tissue was examined by micro-computed tomography (CT) image analysis and histological observation.

2 Materials and methods

2.1 Fabrication of β-TCP/RCP

β-TCP/RCP was fabricated according to the method of Furihata *et al*. [20]. An RCP solution (7.5%,

Cellnest; Fujifilm Wako Pure Chemical Corp., Osaka, Japan) was lyophilized and granulated using a granulator (Quadroco Mill U5; Quadro Engineering, Waterloo, Canada) into particles approximately 1 mm in diameter. RCP granules were then thermally cross-linked at 142°C for 5 hours and dried using a vacuum drying oven (DP-43; Yamato Scientific Co., Ltd., Tokyo, Japan). The size of RCP granules was measured by an automated particle size analyzer (Morphologi G3; Malvern Panalytical Ltd., Malvern, UK), to confirm d_{10}: 0.835 mm, d_{50}: 1.171 mm, and d_{90}: 1.419 mm.

Next, β-TCP (β-TCP-100 milled product; Taihei Chemical Industrial Co., Ltd., Osaka, Japan) was dispersed in water using a wet pulverization/dispersion device (Nanovator NVL-AS200-D10; Yoshida Kikai Co., Ltd., Nagoya, Japan). The particle size distribution of β-TCP was measured using a laser diffraction particle size analyzer (SALD-2100; Shimadzu Corporation, Kyoto, Japan), to confirm d_{10}: 0.452 μm, d_{50}: 0.697 μm, and d_{90}: 1.319 μm. Subsequently, 500 μL of β-TCP dispersion (1 wt%) was added to 100 mg of RCP granules to swell and form β-TCP/RCP (Figure 1A).

2.2 Implantation of β-TCP/RCP to experimental periodontal tissue defects

Five healthy 10-month-old female beagle dogs (Kitayama Labes Co., Ltd., Ina, Japan), weighing approximately 9 to 10 kg, were used in the experiments. After general and local anesthesia [19], mandibular fourth premolars (both left and right side) of the beagle dogs were extracted, and an 8-week preoperative period was allowed for alveolar bone healing of the extraction socket. After healing, a mucoperiosteal flap was made and a three-walled intrabony defect (mesiodistal width × buccolingual width × depth: 5 mm × 3 mm × 4 mm) was created on the mesial side of the left and right mandibular first molar using a dental carbide bar (GC Corporation, Tokyo, Japan) at 3000 rpm (Figure 1B) [21]. The mesial surface of the mesial root of the first molar was planed using a tooth planing bar (Dentech Corporation, Tokyo, Japan) to fully remove the alveolar bone and periodontal ligament tissue to be exposed in the bone defect. Subsequently, one defect was filled with 50 mg of β-TCP/RCP (designated as the β-TCP/RCP group, Figure 1C) and the other defect was left empty (designated as the control group). The defects were completely covered with a mucoperiosteal flap with suturing.

2.3 Micro-CT imaging and bone volume measurement

At 4 weeks (N=2) and 8 weeks (N=3) postoperatively, the dogs were subjected to general anesthesia, euthanized and fixed via perfusion by 10% formalin (Mildform 10N; Fujifilm Wako Pure Chemical Corp.). The tissue blocks were removed, and the bone defects were imaged using a micro-CT (Latheta LCT-200; Hitachi, Ltd., Tokyo, Japan) to observe bone formation. In addition, the amount of new bone in 8-week specimens was quantified using imaging software (ImageJ; National Institutes of Health, Bethesda, MD, USA). After setting up a region of interest (ROI) of 5 mm × 4 mm (mesiodistal width × depth), the bone trabecular area was measured from a series of 30 buccolingual micro-CT images. The sum of the measurements was defined as the bone volume, and the percentage of the total volume of

the ROI was calculated (BV/TV).

2.4 Histological Observations

Tissue blocks were demineralized with 10% ethylenediaminetetraacetic acid and paraffin-embedded according to the conventional method. After slicing in the mesiodistal plane, sections were stained with hematoxylin eosin (HE), Masson's trichrome (MT), and tartaric acid-resistant acid phosphatase (TRAP). In addition, specific antibodies were used to identify osteocalcin (OCN), CD3, CD204, and periostin (POSTIN). After the epitope retrieval step, sections were incubated overnight with primary antibodies: mouse anti-OCN (Takara Bio, Shiga, Japan), mouse anti-CD3 (Agilent Technologies Inc., Santa Clara, CA, USA), mouse anti-CD204 (Cosmo Bio Co., Ltd., Tokyo, Japan) and rabbit anti-POSTIN (Abcam plc., Cambridge, UK). The antigen-antibody reaction sites were visualized using diaminobenzidine. The stained sections were observed using an optical microscope (NanoZoomer S210; Hamamatsu Photonics K.K., Shizuoka, Japan).

2.5 Histometric measurements

Using MT-stained and POSTIN-stained images at 8 weeks after surgery and imaging software, the following properties were measured: (1) gingival tissue height (distance from the bottom of the defect to the most coronally oriented point of the gingival tissue), (2) junctional epithelium height (distance from the bottom of the defect to the most apical position of the junctional epithelium), (3) new bone height (distance from the bottom of the defect to the most coronally oriented point of new bone-like tissue), (4) POSTIN expression tissue height (distance from the bottom of the defect to the most coronally oriented point of the POSTIN-expressing tissue).

2.6 Statistical analysis

The values of micro-CT and histometric measurements of the β-TCP/RCP and control (Ctrl) groups were statistically analyzed using the two-tailed Mann-Whitney U test. P-values of <0.05 were considered statistically significant. Statistical procedures were performed using the SPSS software package (version 11.0; IBM Corp., Armonk, NY, USA).

3 Results

3.1 Evaluation by micro-CT imaging

Figure 2A shows micro-CT images of periodontal tissue defects. At 4 weeks, the β-TCP/RCP group showed slight formation of new bone (radiopaque area) at the bottom of the bone defect (indicated by the yellow dashed line). In the Ctrl group, slight formation of new bone was shown in the bone defect, similar to the β-TCP/RCP group. The vertical height of the mesial wall of the bone defect (arrows) in the Ctrl group tended to be lower than in the β-TCP/RCP group. Micro-CT images of the 8-week β-TCP/RCP

group showed that most of the bone defect was filled with newly formed bone. Notably, a periodontal ligament-like space (no direct contact between alveolar bone and root) existed between the new bone and the tooth root. The vertical height of the mesial wall of the bone defect was maintained as in the 4-week group. In contrast, although the opaque density increased in the Ctrl group, only slight bone formation was observed in the defect. Moreover, the upper region of the bone defect area showed radiolucency, and the mesial wall of the bone defect was low as in the 4-week group.

Quantitative evaluation of bone volume at 8 weeks postoperatively showed that the mean ± standard deviation of new bone volume ($\times 10^4$ pixels) was 12.9 ± 3.5 and 6.0 ± 2.1 in the β-TCP/RCP group and Ctrl group, respectively. The β-TCP/RCP group had approximately 2.2-fold more new bone than the Ctrl group, and there was a significant difference between the two groups ($P<0.05$) (Figure 2B).

3.2 Histological observation at 4 weeks

Figure 3 shows MT-stained and OCN immunostained sections at 4 weeks postoperatively (the left column of Supplemental Figure shows HE-stained sections at 4 weeks). New bone-like tissue was formed continuously from the pre-existing alveolar bone in the β-TCP/RCP area remaining in the defect (Figure 3A). The defect region containing residual β-TCP/RCP and bone-like tissue was covered by fibrous tissue (FT) derived from the gingiva on the coronal side, and the downgrowth of the junctional epithelium was arrested at the cement-enamel junction (Figure 3B, arrows). Cross-sections of the residual β-TCP/RCP showed reticular structures of non-uniform size, and dark blue-stained new bone-like tissue was found in the inner regions of the reticular structures (Figure 3C). Residual β-TCP/RCP granules close to the root or gingiva tended to show less bone-like tissue formation in and around the granules. Although there was no ankylosis between the root surface and the new bone-like tissue, the formation of periodontal ligament-like tissue was not clear due to residual β-TCP/RCP (Figure 3C). OCN immunostaining was performed to confirm the presence of osteoblastic cells around the newly formed bone. OCN-positive cells (dark brown) were observed close to the newly formed bone-like tissue in the reticular structure of the β-TCP/RCP group (Figure 3D). In the Ctrl group at 4 weeks postoperatively, new bone-like tissue was formed in the defect area that was continuous with the pre-existing bone, which has rich bone trabeculae (Figure 3E). The gingival fibrous tissue was close to the root surface and filled most of the defect, while the junctional epithelium grew down along the root surface to the center of the defect (arrows in Figure 3F), with no periodontal ligament-like tissue formation (Figure 3F).

Figure 4 shows the results of TRAP, CD3, CD204, and POSTIN immunostaining at 4 weeks postoperatively. TRAP staining showed that TRAP-positive osteoclastic cells (red) were frequently observed around the bone-like tissue formed by β-TCP/RCP implantation, especially in the region adjacent to the pre-existing bone, but rarely on the gingival side. In the Ctrl group, the expression of TRAP-positive cells was especially high in the superficial area of the new bone-like tissue. CD3-positive lymphocytes (dark brown) were only found in the gingival fibrous tissue adjacent to the gingival sulcus

on the coronal side in both groups (probably due to attack by periodontal pocket flora) and were negative around the implanted β-TCP/RCP. The distribution of CD204-positive macrophages (dark brown) was distinctive; they were detected in association with the β-TCP/RCP residues in the defect, especially in the area close to the gingival fibrous tissue. In addition, strong positive expression was also observed in residues of β-TCP/RCP close to the root surface. In contrast, CD204 staining was negative in the control group. POSTIN was expressed (dark brown) in the pre-existing periodontal ligament and in the space between the root and the new bone-like tissue. In the coronal region of the defect, POSTIN expression was weak, and was especially negative in the area of epithelial downgrowth (arrows) in the control group.

3.3 Histological observation at 8 weeks

Figure 5 shows MT-stained and OCN-immunostained sections at 8 weeks postoperatively (the right panel in Supplementary Figure shows HE-stained sections at 8 weeks). In the β-TCP/RCP group, β-TCP/RCP remained in the defect as observed at 4 weeks; however, its shape and internal structure were unclear, and much bone-like tissue was observed within the β-TCP/RCP implantation region. Downgrowth of the junctional epithelium stopped around the tooth cervical region (Figure 5A). Periodontal ligament-like tissue was found in the space between the root and the new bone-like tissue, and was continuous with the pre-existing periodontal ligament. No ankylosis was observed in this study (Figure 5B). Residual β-TCP/RCP was also scattered within the gingival fibrous tissue, and no bone-like tissue formation was observed in the surrounding areas, with fibrous tissue invading the granules (Figure 5C). OCN immunostaining indicated that OCN-positive cells were present around the bone-like tissue found around the β-TCP/RCP, as observed at 4 weeks (Figure 5D).

Figure 6 shows the results of TRAP, CD3, CD204, and POSTIN immunostaining at 8 weeks postoperatively. In contrast to 4 weeks postoperatively, TRAP-positive cells in the β-TCP/RCP group were dispersed throughout the bone defect and were particularly strongly observed at the borders between the bone-like tissue and gingival fibrous tissue (arrows) or periodontal ligament-like tissue. In the control group, TRAP-positive cells were also found in the bone-like tissue located close to the periodontal ligament-like tissue. CD3-positive cells were located within the fibrous tissue of the free gingiva in both groups as at 4 weeks and were not observed around the residual β-TCP/RCP. CD204-positive cells were found around the residual β-TCP/RCP; however, CD204 expression tended to be lower compared to that at 4 weeks. CD204 staining was negative in the control group. POSTIN staining revealed expression between the root and the new bone-like tissue that continued to the pre-existing periodontal ligament in both groups. Some fiber bundle structures were observed between the root surface and the new bone-like tissue.

3.4 Histological measurements

Histological measurements of the stained images at 8 weeks revealed that in the β-TCP/RCP and Ctrl groups, the gingival tissue height was 4.9 ± 0.7 mm and 3.1 ± 0.7 mm, junctional epithelium height was 3.7 ± 0.2 mm and 2.7 ± 0.5 mm, new bone height was 2.2 ± 0.2 mm and 1.3 ± 0.2 mm, and POSTIN expression tissue height was 2.8 ± 1.0 mm and 1.4 ± 0.2 mm, respectively. These values for the β-TCP/RCP group were approximately 1.6-, 1.3-, 1.7-, and 2.1-fold higher than the Ctrl group, respectively, and significant differences were detected between the two groups for all parameters ($P<0.05$) (Figure 7).

4 Discussion

Quantitative analysis using micro-CT images at 8 weeks postoperatively showed that the β-TCP/RCP group had a significantly greater amount of new bone (radiopaque area) than the Ctrl group (Figure 2A and 2B). The radiopaque areas were generally consistent with the MT-stained new bone-like tissue areas (Figures 3 and 5) and the large number of OCN-positive osteoblast-like cells. Furthermore, histological measurements showed that the β-TCP/RCP group had significantly greater new bone height than the Ctrl group (Figure 7). These results suggest that β-TCP/RCP implantation promoted bone healing. Furihata *et al*. reported that co-culture of β-TCP/RCP and osteoblast-like cells promoted mRNA expression of osteogenic markers (runt-related transcription factor 2, alkaline phosphatase, and bone sialoprotein) to simultaneously stimulate integrin β1 expression [20]. Integrin-mediated cell adhesion to extracellular matrix components, such as type I collagen, is known to activate focal adhesion kinase and its downstream target, bone morphogenetic protein-smad signaling, which is involved in promoting osteoblast differentiation [22]. Since genetic engineering was used to design β-TCP/RCP to contain many RGD sequences [7, 8], it is expected that integrin-mediated cell adhesion would frequently occur *in vivo*, thereby promoting osteoblast differentiation and bone formation at the β-TCP/RCP implantation site. In addition, calcium and phosphate ions released from β-TCP reportedly play a major role in bone formation [23, 24]. Increasing inorganic phosphate concentrations inhibited osteoclast differentiation and bone resorption activity [25]. It was a distinctive finding that TRAP-positive cells were localized at the base of the bone defect at week 4, whereas high expression was detected throughout the whole defect at week 8 (Figures 4 and 6). Hence, it seems likely that the large amount of calcium and phosphate ions released from the β-TCP submicron particles in the early stage of osteogenesis caused early bone tissue deposition and suppression of osteoclasts to consequently promote bone formation.

In periodontal regenerative therapy, it is generally considered beneficial to inhibit downgrowth of the junctional epithelium, thereby maintaining the regenerative space until bone is formed [26]. Micro-CT images at 4 weeks after surgery showed radiolucency (presumably no bone formation) in the coronal region of the defects in both the β-TCP/RCP and Ctrl groups (Figure 2A). However, based on the evidence described below, we speculate that the β-TCP/RCP implantation prevents epithelial downgrowth and maintains the regenerative space, although bone regeneration after 4 weeks is still insufficient. (i)

Histological observations at 4 weeks showed that the grafted β-TCP/RCP (not visible on X-ray) filled the defect in the β-TCP/RCP group, whereas gingival fibrous tissue filled most of the defect in the Ctrl group (Figure 3A and 3E). (ii) The Ctrl group showed epithelial downgrowth to the middle of the defect (Figure 3F) and failed to maintain the height of the mesial wall of the surgically created bone defect (Figures 2A and 3E). (iii) Histological measurements showed significantly higher junctional epithelial height in the β-TCP/RCP group compared to the Ctrl group (Figure 7). On the other hand, RCP promotes proliferation of several types of cells, such as mesenchymal stromal cells [27] and synovial mesenchymal cells [28]. In the present study, β-TCP/RCP was found in the gingival fibrous tissue 8 weeks after implantation (Figure 5C), however, these β-TCP/RCP granules were not related to osteogenesis. The ability of β-TCP/RCP to induce mesenchymal cell proliferation was limited in the gingival fibrous tissue. For example, in severe periodontitis with large bone lesions, β-TCP/RCP is presumably less prone to ectopic bone formation beyond the region surrounded by bone walls.

Since the periodontal ligament is an important structure involved in mastication, it should be regenerated at the same time as alveolar bone formation in periodontal tissue regeneration therapy [29]. When biomaterials that strongly regenerate bone are implanted, adhesion between the new bone and the root of the tooth (ankylosis) may be observed without formation of the periodontal ligament [30]. In the present study, no ankylosis was observed and POSTIN-positive fibrous tissue along the root was shown in the β-TCP/RCP group (Figures 4 and 6). POSTIN is a secreted matricellular protein that is commonly expressed in the periodontal ligament or periosteum [31, 32] and is a marker for periodontal ligament regeneration [33, 34, 35]. Therefore, POSTIN-positive regions in the β-TCP/RCP group may represent the periodontal ligament or its precursor tissue, suggesting regeneration of the periodontal ligament following β-TCP/RCP grafting. Cementum regeneration, which serves as an anchor for fiber bundles, is important for periodontal ligament regeneration [36]; unfortunately, no obvious cementum formation was identified in the present study [3, 30, 37]. However, β-TCP/RCP remained in the regeneration site at 8 weeks after implantation, suggesting that further remodeling may subsequently occur to reconstruct the periodontal apparatus.

The implantation site of periodontal tissue regenerative materials is constantly exposed to the risk of infection by oral bacteria because of its location close to the oral cavity [38]. Therefore, rapid resorption and tissue replacement of the grafted material are required. In this study, the mesh structure of residual β-TCP/RCP gradually became sparse by 8 weeks, and CD204-positive M2 macrophage expression was observed around β-TCP/RCP granules, suggesting that the residual β-TCP/RCP was undergoing resorption. There was almost no accumulation of CD3-positive cells to β-TCP/RCP, suggesting that there is no concern about detrimental inflammatory reactions against periodontal tissue regeneration caused by residual β-TCP/RCP [39]. In addition, bioceramics such as β-TCP are non-absorbable, or must remain *in vivo* for more than a half year to be absorbed and can inhibit tissue replacement [40, 41]. In this project, β-TCP was added to promote bone formation through ion supply, but

was adjusted to a submicron size to ensure smooth resorption. As a result, no residual β-TCP was observed histologically, which is consistent with previous reports [20] and suggests that it does not produce long-term effects on tissue replacement and periodontal regeneration.

5 Conclusions

After β-TCP/RCP was implanted into experimental periodontal tissue defects, the effect of periodontal tissue healing was assessed in beagle dogs. Micro-CT analysis showed that the amount of new bone in the β-TCP/RCP group was significantly greater (2.2-fold) than in the Ctrl group at 8 weeks postoperatively. Histological findings showed the formation of bone-like and periodontal ligament-like tissue at the β-TCP/RCP implantation site. Histological measurements revealed that the periodontal tissue regeneration parameters in the β-TCP/RCP group were significantly greater than those in the Ctrl group. These results suggest that β-TCP/RCP is an effective material for promoting periodontal tissue regeneration.

Acknowledgments

This study was supported by Hokkaido University, which provided facilities and resources. β-TCP and RCP were kindly provided by Taihei Chemical Industrial Co., Ltd. and FUJIFILM Corp., respectively.

CRediT authorship contribution statement

YY: methodology, validation, formal analysis, investigation, writing - original draft, visualization. HM: conceptualization, methodology, validation, formal analysis, investigation, writing - original draft, visualization, supervision. EN: validation, investigation. YK: investigation. AH: investigation. AK: validation, investigation, writing - review & editing. TS: resources, writing - review & editing. TA: investigation, writing - review & editing. All of the authors have approved the final version of the manuscript.

Conflicts of Interest

All authors have no conflicts of interest to disclose for this study.

Ethics Approval

Animal experiments were conducted in accordance with the institutional animal use and care regulations of Hokkaido University (Animal Research Committee of Hokkaido University, Approval number 19-84) and approved by the Animal Research Committee of Hokkaido University. Experiments on animals were carried out in accordance with relevant guidelines and regulations.

Funding

This research was supported by JSPS KAKENHI (Grant Nos. JP16K11822 and JP22K10012) and the 2020 AMED Translational Research Program (Grant No. A154).

Data Availability Statement

The datasets are available from the corresponding author upon reasonable request.

References

1) T. Iwata, M. Yamato, H. Tsuchioka, R. Takagi, S. Mukobata, K. Washio, et al. Periodontal regeneration with multi-layered periodontal ligament-derived cell sheets in a canine model. Biomaterials, 30 (2009), pp. 2716-2723.

2) C. Vaquette, S.P. Pilipchuk, P.M. Bartold, D.W. Hutmacher, W.V. Giannobile, S. Ivanovski. Tissue engineered constructs for periodontal regeneration: current status and future perspectives. Adv Healthc Mater, 7 (2018), p. e1800457.

3) Y. Shirakata, T. Nakamura, Y. Shinohara, K. Nakamura-Hasegawa, C. Hashiguchi, N. Takeuchi, et al. Split-mouth evaluation of connective tissue graft with or without enamel matrix derivative for the treatment of isolated gingival recession defects in dogs. Clin Oral Investig, 23 (2019), pp. 3339-3349.

4) A.M. Ferreira, P. Gentile, V. Chiono, G. Ciardelli. Collagen for bone tissue regeneration. Acta Biomater, 8 (2012), pp. 3191-3200.

5) Y. Kosen, H. Miyaji, A. Kato, T. Sugaya, M. Kawanami. Application of collagen hydrogel/sponge scaffold facilitates periodontal wound healing in class II furcation defects in beagle dogs. J Periodont Res, 47 (2012), pp. 626-634.

6) J.A. Ramshaw. Biomedical applications of collagens. J Biomed Mater Res B Appl Biomater, 104 (2016), pp. 665-675.

7) K.M. Pawelec, D. Confalonieri, F. Ehlicke, H.A. van Boxtel, H. Walles, S.G.J.M. Kluijtmans. Osteogenesis and mineralization of mesenchymal stem cells in collagen type I-based recombinant peptide scaffolds. J Biomed Mater Res A, 105 (2017), pp. 1856-1866.

8) M. Parvizi, J.A. Plantinga, C.A. van Speuwel-Goossens, E.M. van Dongen, S.G. Kluijtmans, M.C. Harmsen. Development of recombinant collagen-peptide-based vehicles for delivery of adipose-derived stromal cells. J Biomed Mater Res A 104 (2016), pp. 503-516.

9) K. Nakamura, R. Iwazawa, Y. Yoshioka. Introduction to a new cell transplantation platform via recombinant peptide petaloid pieces and its application to islet transplantation with mesenchymal stem cells. Transpl Int. 29 (2016), pp. 1039-1050.

10) Y. Akiyama, M. Ito, T. Toriumi, T. Hiratsuka, Y. Arai, S. Tanaka, et al. Bone formation potential of collagen type I-based recombinant peptide particles in rat calvaria defects. Regen Ther, 16 (2020), pp. 12-22.

11) M. Miyamoto, K. Nakamura, H. Shichinohe, T. Yamauchi, M. Ito, H. Saito, et al. Human recombinant peptide sponge enables novel.; Less invasive cell therapy for ischemic stroke. Stem Cells Int. 2018 (2018), p. 4829534.

12) T. Mashiko, H. Takada, S.H. Wu, K. Kanayama, J. Feng, K. Tashiro, et al. Therapeutic effects of a recombinant human collagen peptide bioscaffold with human adipose-derived stem cells on impaired wound healing after radiotherapy. J Tissue Eng Regen Med, 12 (2018), PP. 1186-1194.

13) D. Zhang, X. Wu, J. Chen, K. Lin. The development of collagen based composite scaffolds for bone regeneration. Bioact Mater, 3 (2017), PP. 129-138.

14) S. Murakami, H. Miyaji, E. Nishida, K. Kawamoto, S. Miyata, H. Takita, et al. Dose effects of beta-tricalcium phosphate nanoparticles on biocompatibility and bone conductive ability of three-dimensional collagen scaffolds. Dent Mater J, 36 (2017), pp. 573-583.

15) K. Ogawa, H. Miyaji, A. Kato, Y. Kosen, T. Momose, T. Yoshida, et al. Periodontal tissue engineering by nano beta-tricalcium phosphate scaffold and fibroblast growth factor-2 in one-wall infrabony defects of dogs. J Periodont Res, 51 (2016), pp. 758-767.

16) S. Oshima, T. Sato, M. Honda, Y. Suetsugu, K. Ozeki, M. Kikuchi. Fabrication of gentamicin-loaded hydroxyapatite/collagen bone-like nanocomposite for anti-infection bone void fillers. Int J Mol Sci, 21 (2020), p. 551.

17) T. Kawai, S. Echigo, K. Matsui, Y. Tanuma, T. Takahashi, O. Suzuki, et al. First clinical application of octacalcium phosphate collagen composite in human bone defect. Tissue Eng Part A, 20 (2014), pp. 1336-1341.

18) S. Santhakumar, A. Oyane, M. Nakamura, Y. Yoshino, M.K. Alruwaili, H. Miyaji. Bone tissue regeneration by collagen scaffolds with different calcium phosphate coatings: amorphous calcium phosphate and low-crystalline apatite. Materials (Basel), 14 (2021), p. 5860.

19) Y. Kanemoto, H. Miyaji, E. Nishida, S. Miyata, K. Mayumi, Y. Yoshino, et al. A. Periodontal tissue engineering using an apatite/collagen scaffold obtained by a plasma- and precursor-assisted biomimetic process. J Periodont Res, 57 (2022), pp. 205-218.

20) T. Furihata, H. Miyaji, E. Nishida, A. Kato, S. Miyata, K. Shitomi, et al. Bone forming ability of recombinant human collagen peptide granules applied with β-tricalcium phosphate fine particles. J Biomed Mater Res B Appl Biomater, 108 (2020), pp. 3033-3044.

21) T. Nagayasu-Tanaka, J. Anzai, S. Takaki, N. Shiraishi, A. Terashima, T. Asano, et al. Action mechanism of fibroblast growth factor-2 (FGF-2) in the promotion of periodontal regeneration in beagle dogs. PLoS One, 10 (2015), p. e0131870..

22) Y. Tamura, Y. Takeuchi, M. Suzawa, S. Fukumoto, M. Kato, K. Miyazono, et al. Focal adhesion kinase activity is required for bone morphogenetic protein—Smad1 signaling and osteoblastic differentiation in murine MC3T3-E1 cells. J Bone Miner Res, 16 (2001), pp. 1772-1779.

23) J. Jeong, J.H. Kim, J.H. Shim, N.S. Hwang, C.Y. Heo. Bioactive calcium phosphate materials and applications in bone regeneration. Biomater Res, 23 (2019), p. 4.

24) Y. Maazouz, I. Rentsch, B. Lu, B.L.G. Santoni, N. Doebelin, M. Bohner, In vitro measurement of the chemical changes occurring within β-tricalcium phosphate bone graft substitutes. Acta Biomater, 102 (2020), pp. 440-457.

25) M. Kanatani, T. Sugimoto, J. Kano, M. Kanzawa, K. Chihara. Effect of high phosphate concentration on osteoclast differentiation as well as bone-resorbing activity. J Cell Physiol, 196 (2003), pp. 180-189.

26) Z. Sheikh, J. Qureshi, A.M. Alshahrani, H. Nassar, Y. Ikeda, M. Glogauer, et al. Collagen based barrier membranes for periodontal guided bone regeneration applications. Odontology, 105 (2017), pp. 1-12.

27) K. Muraya, T. Kawasaki, T. Yamamoto, H. Akutsu. Enhancement of cellular adhesion and proliferation in human mesenchymal stromal cells by the direct addition of recombinant collagen I peptide to the culture medium. Biores Open Access, 8 (2019), pp. 210-218.

28) M. Naritomi, M. Mizuno, H. Katano, N. Ozeki, K. Otabe, K. Komori, et al. Petaloid recombinant peptide enhances in vitro cartilage formation by synovial mesenchymal stem cells. J Orthop Res, 37 (2019), pp. 1350-1357.

29) M. Bousnaki, A. Beketova, E. Kontonasaki. A review of in vivo and clinical studies applying scaffolds and cell sheet technology for periodontal ligament regeneration. Biomolecules, 12 (2022), p. 435.

30) D. Takahashi, T. Odajima, M. Morita, M. Kawanami, H. Kato. Formation and resolution of ankylosis under application of recombinant human bone morphogenetic protein-2 (rhBMP-2) to class III furcation defects in cats. J Periodont Res, 40 (2005), pp. 299-305.

31) K. Horiuchi, N. Amizuka, S. Takeshita, H. Takamatsu, M. Katsuura, H. Ozawa, et al. Identification and characterization of a novel protein.; periostin.; with restricted expression to periosteum and periodontal ligament and increased expression by transforming growth factor beta. J Bone Miner Res, 14 (1999), pp. 1239-1249.

32) J. Du, M. Li. Functions of periostin in dental tissues and its role in periodontal tissues' regeneration. Cell Mol Life Sci, 74 (2017), pp. 4279-4286.

33) C.H. Park, H.F. Rios, Q. Jin, J.V. Sugai, M. Padial-Molina, A.D. Taut, et al. Tissue engineering bone-ligament complexes using fiber-guiding scaffolds. Biomaterials, 33 (2012), pp. 137-145.

34) S.P. Pilipchuk, T. Fretwurst, N. Yu, L. Larsson, N.M. Kavanagh, F. Asa'ad, et al. Micropatterned scaffolds with Immobilized growth factor genes regenerate bone and periodontal ligament-like tissues. Adv Healthc Mater, 7 (2018), p. e1800750.

35) A. Basu, K. Rothermund, M.N. Ahmed, F.N. Syed-Picard. Self-assembly of an organized cementum-periodontal ligament-like complex using scaffold-free tissue engineering. Front Physiol, 10 (2019), p. 422.

36) H. Arzate, M. Zeichner-David, G. Mercado-Celis. Cementum proteins: role in cementogenesis.; biomineralization.; periodontium formation and regeneration. Periodontol 2000, 67 (2015), pp. 211-233.

37) J. Anzai, T. Nagayasu-Tanaka, A. Terashima, T. Asano, S. Yamada, T. Nozaki, et al. Long-term observation of regenerated periodontium induced by FGF-2 in the beagle dog 2-wall periodontal defect model. PLoS One, 11 (2016), p. e0158485.

38) N.B. Arweiler, L. Netuschil. The oral microbiota. Adv Exp Med Biol, 902 (2016), pp. 45-60.

39) H. Katagiri, L.F. Mendes, F.P. Luyten. Reduction of BMP6-induced bone formation by calcium phosphate in wild-type compared with nude mice. J Tissue Eng Regen Med, 13 (2019), pp. 846-856.

40) K. Kurashina, H. Kurita, Q. Wu, A. Ohtsuka, H. Kobayashi. Ectopic osteogenesis with biphasic ceramics of hydroxyapatite and tricalcium phosphate in rabbits. Biomaterials, 23 (2002), pp. 407-412.

41) S. Kamakura, Y. Sasano, T. Shimizu, K. Hatori, O. Suzuki, M. Kagayama, et al. Implanted octacalcium phosphate is more resorbable than beta-tricalcium phosphate and hydroxyapatite. J Biomed Mater Res, 59 (2002), pp. 29-34.

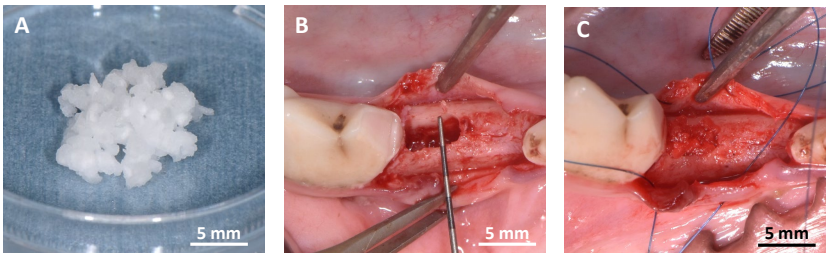

Figure 1. Surgical procedure of β-TCP/RCP granule implantation

(A) Digital photograph of β-TCP/RCP granules. (B) Surgically created 3-wall intrabony defect. (C) Placement of β-TCP/RCP into the defect.

Abbreviations: RCP, recombinant human collagen peptide; TCP, tricalcium phosphate.

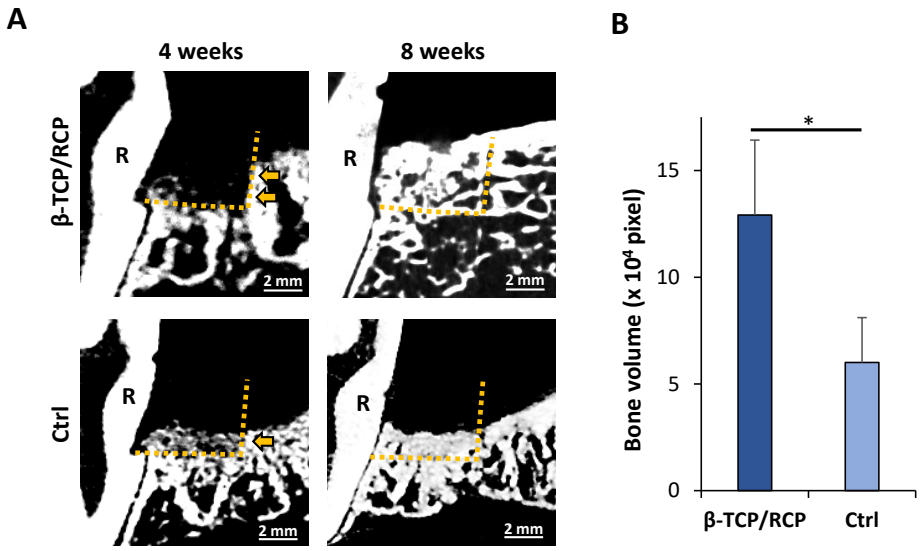

Figure 2. Micro-CT analysis

(A) Micro-CT images of a mesiodistal cross section of bone defects. The yellow dashed lines and arrows indicate the border of the bone defect and the mesial bone wall, respectively. (B) Bone volume (n = 3, mean ± standard deviation). *: $P < 0.05$. Statistical analysis: two-tailed Mann-Whitney U test.

Abbreviations: CT, computed tomography; Ctrl, control; R, root; RCP, recombinant human collagen peptide; TCP, tricalcium phosphate.

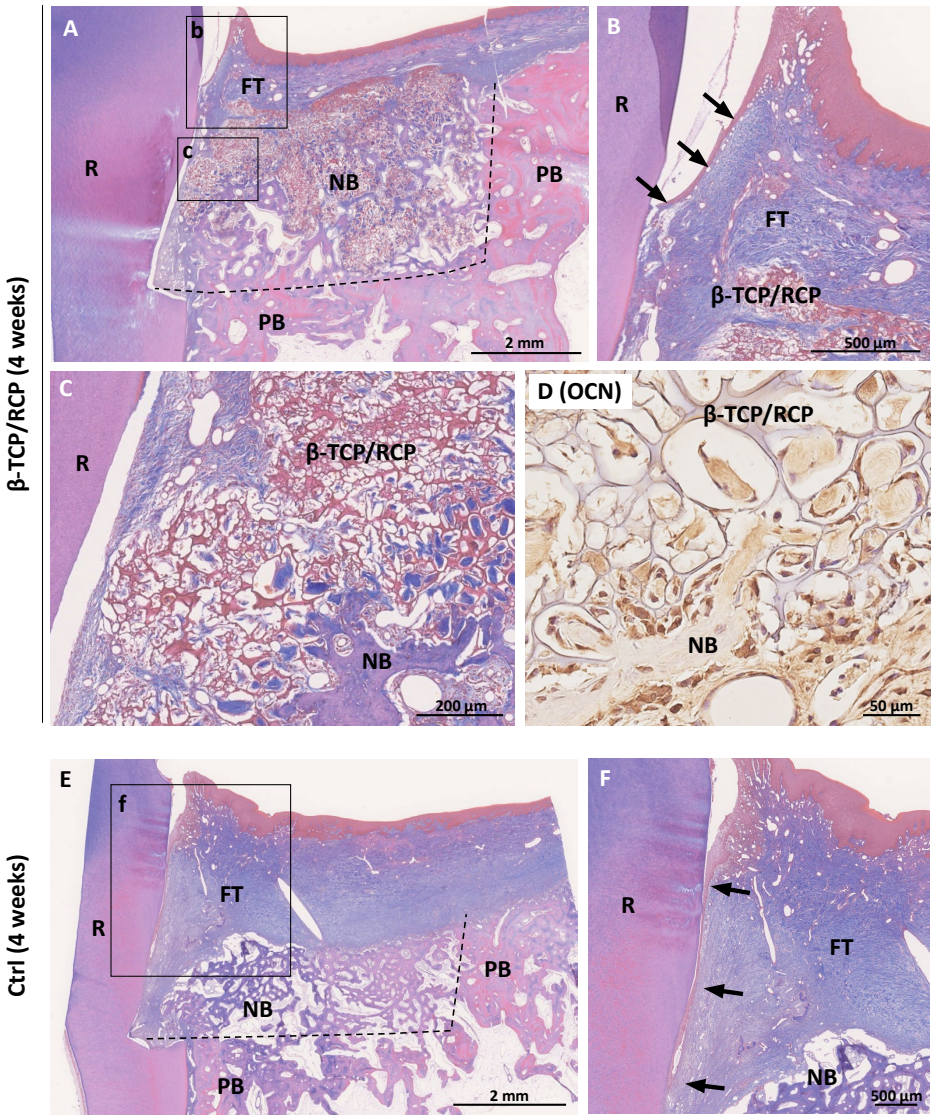

Figure 3. Histological findings at 4 weeks

(A) Histological image of a β-TCP/RCP group specimen. (B) Higher magnification image related to framed area (b) in panel A. Arrows indicate junctional epithelium. (C) Higher magnification image related to framed area (c) in panel A. (D) OCN-positive cells (dark brown) related to β-TCP/RCP and new bone-like tissue. (E) Histological image of a Ctrl group specimen. (F) Higher magnification image related to framed area (f) in panel E. Arrows indicate junctional epithelium. (A-C, E, F) Masson trichrome staining, (D) OCN immunostaining. The black dashed lines indicate the border of the bone defects.

Abbreviations: Ctrl, control; FT, fibrous tissue; NB, new bone-like tissue; OCN, osteocalcin; PB, pre-existing bone; R, root; RCP, recombinant human collagen peptide; TCP, tricalcium phosphate.

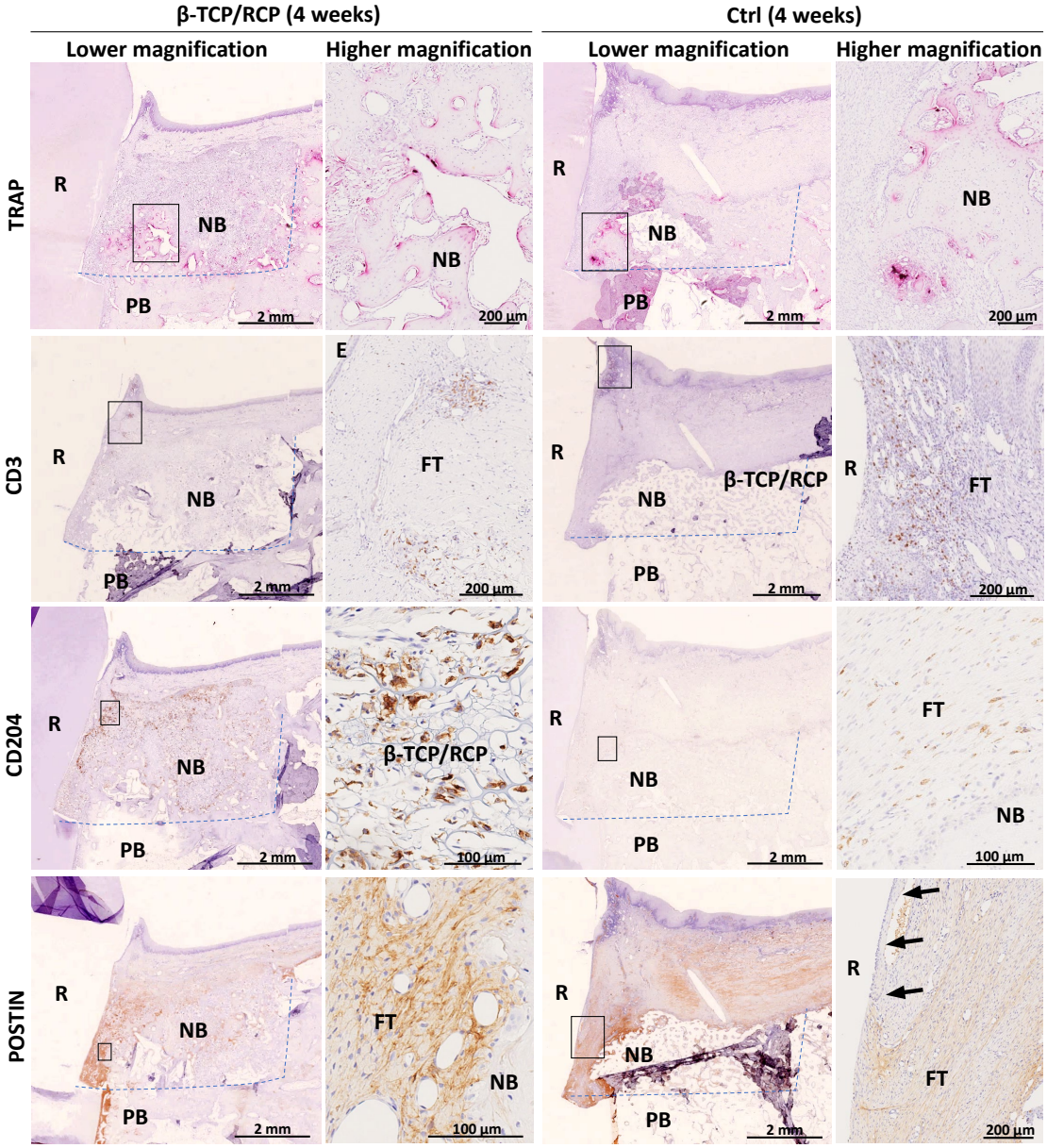

Figure 4. TRAP staining (red) and CD3, CD204 and POSTIN immunostaining (dark brown) at 4 weeks

The high-magnification image in the right column of each group shows the framed area in the adjacent low-magnification image in the left column. Arrows in POSTIN staining of the Ctrl group indicate the junctional epithelium. The blue dashed lines indicate the border of the bone defects.

Abbreviations: Ctrl, control; FT, fibrous tissue; NB, new bone-like tissue; PB, pre-existing bone; POSTIN, periostin; R, root; RCP, recombinant human collagen peptide; TCP, tricalcium phosphate; TRAP, tartaric acid-resistant acid phosphatase.

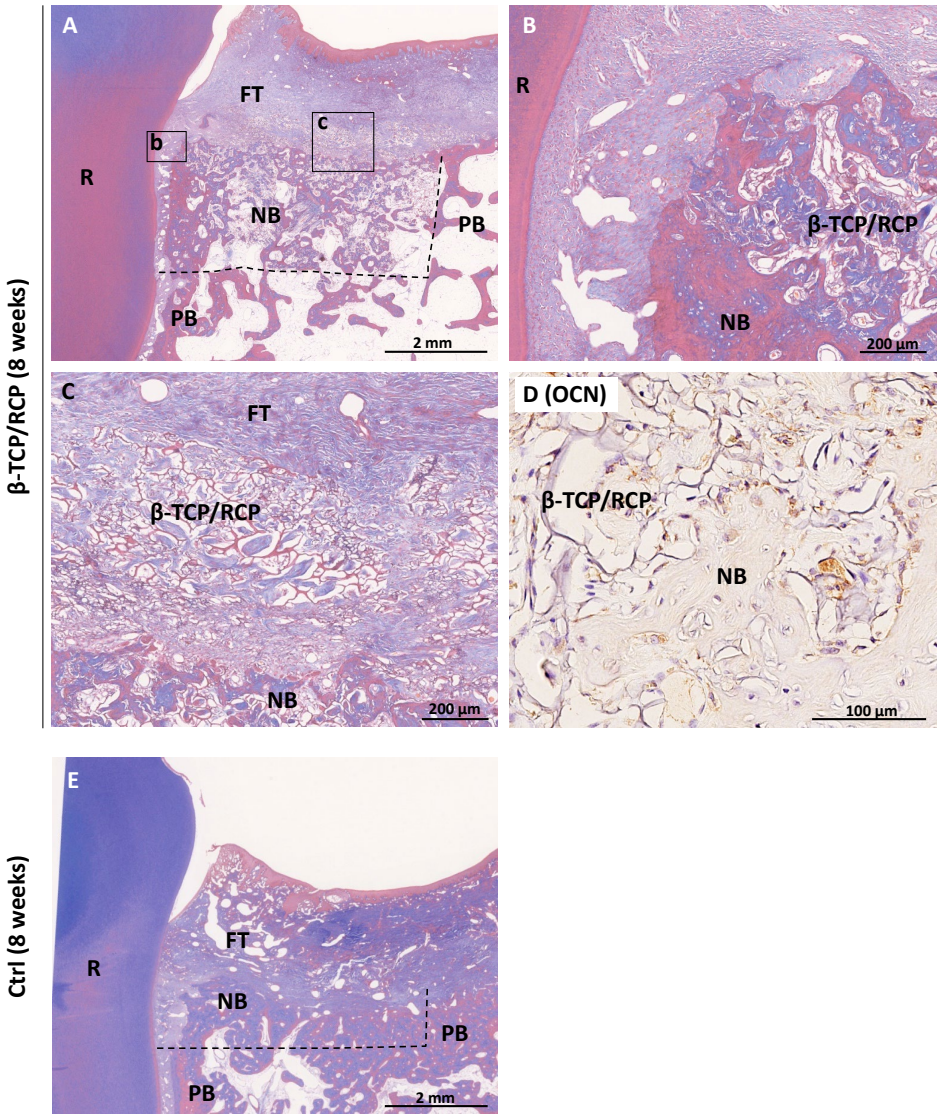

Figure 5. Histological findings at 8 weeks

(A) Histological image of a β-TCP/RCP group specimen. (B) Higher magnification image related to framed area (b) in panel A. (C) Higher magnification image related to framed area (c) in panel A. (D) OCN-positive cells (dark brown) related to β-TCP/RCP and new bone-like tissue. (E) Histological image of a Ctrl group specimen. (A-C, E) Masson trichrome staining, (D) OCN immunostaining. The black dashed lines indicate the border of the bone defects.

Abbreviations: Ctrl, control; FT, fibrous tissue; NB, new bone-like tissue; OCN, osteocalcin; PB, pre-existing bone; R, root; RCP, recombinant human collagen peptide; TCP, tricalcium phosphate.

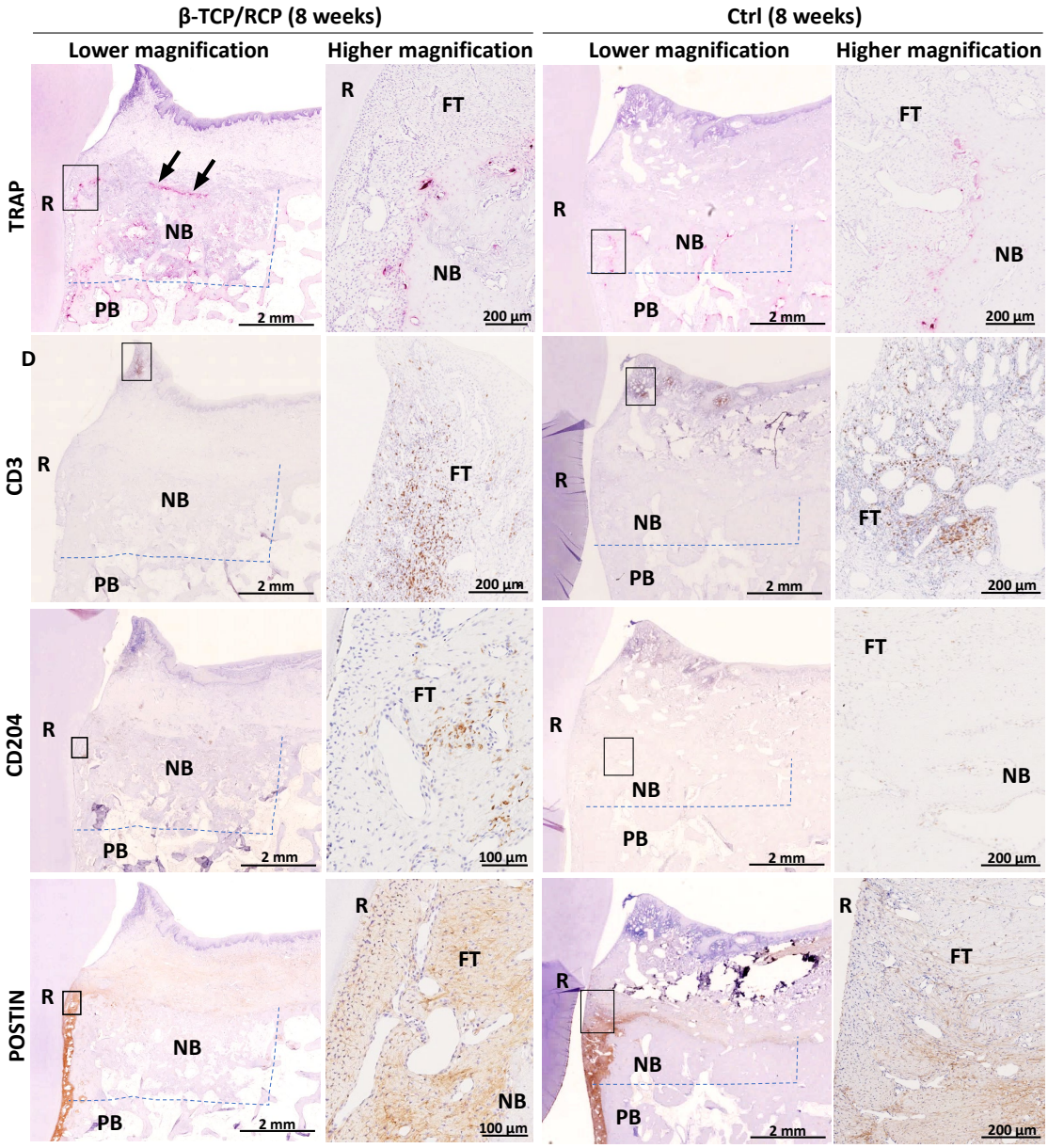

Figure 6. TRAP staining (red) and CD3, CD204 and POSTIN immunostaining (dark brown) at 8 weeks

The high-magnification image in the right column of each group shows the framed area in the adjacent low-magnification image in the left column. Arrows in TRAP staining of the β-TCP/RCP group indicate that TRAP-positive cells were close to gingival fibrous tissue. The blue dashed lines indicate the border of the bone defects.

Abbreviations: Ctrl, control; FT, fibrous tissue; NB, new bone-like tissue; PB, pre-existing bone; POSTIN, periostin; R, root; RCP, recombinant human collagen peptide; TCP, tricalcium phosphate; TRAP, tartaric acid-resistant acid phosphatase.

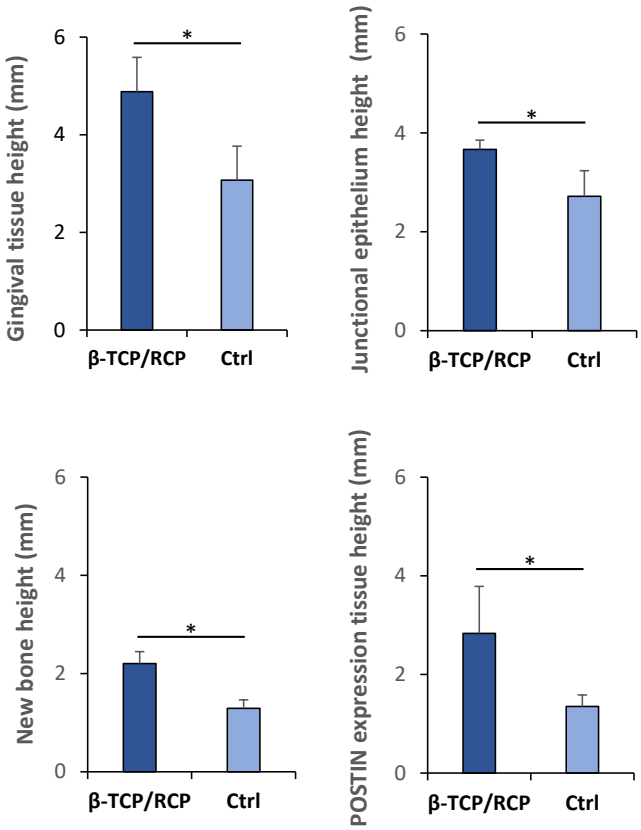

Figure 7. Results of histometric measurements

The height of gingival tissue, junctional epithelium, new bone and POSTIN expression tissue (n = 3, mean ± standard deviation). *: $P < 0.05$. Statistical analysis: two-tailed Mann-Whitney U test.

Abbreviations: Ctrl, control; POSTIN, periostin; RCP, recombinant human collagen peptide; TCP, tricalcium phosphate.

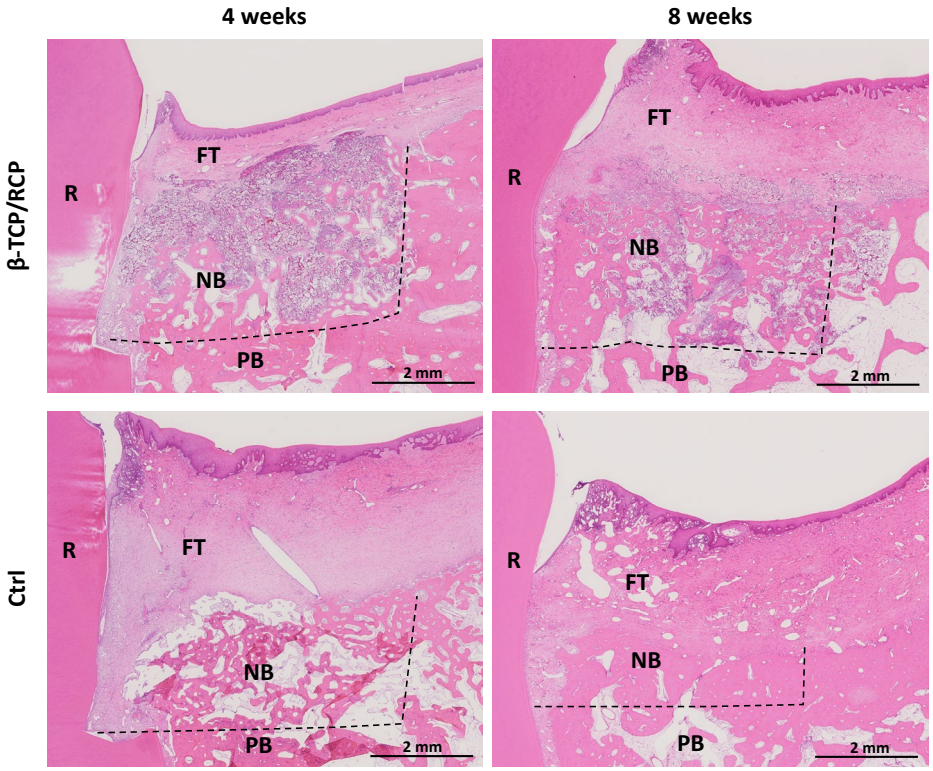

Supplementary Figure. HE stained sections

The black dashed lines indicate the border of the bone defects.

Abbreviations: Ctrl, control; FT, fibrous tissue; NB, new bone-like tissue; PB, pre-existing bone; R, root; RCP, recombinant human collagen peptide; TCP, tricalcium phosphate.